



Journal Name

## COMMUNICATION

# Expanding the light absorption of poly(3-hexylthiophene) by end-functionalization with $\pi$ -extended porphyrins

Received 00th January 20xx,  
Accepted 00th January 20xx

Michèle Chevrier,<sup>a,b</sup> Sébastien Richeter,<sup>a</sup> Olivier Coulembier,<sup>b</sup> Mathieu Surin,<sup>c</sup> Ahmad Mehdi,<sup>a</sup>  
Roberto Lazzaroni,<sup>c</sup> Rachel C. Evans,<sup>d,e</sup> Philippe Dubois<sup>b</sup> and Sébastien Clément<sup>a,\*</sup>

DOI: 10.1039/x0xx00000x

www.rsc.org/

**Poly(3-hexylthiophene)s end-functionalized with  $\pi$ -extended porphyrins have been synthesized in a one-pot procedure. The polymers show a broad absorption profile extending to 700 nm and a fibrillar microstructure, which can be tuned through judicious selection of the porphyrin molar ratio.**

The development of new conjugated polymers is a major route to improve the power conversion efficiency (PCE) of bulk heterojunction (BHJ)-type polymer solar cells (PSCs), making them one of the most promising candidates as renewable energy sources.<sup>1</sup> In this context, considerable attention has been paid to BHJ-PSCs based on poly(3-hexylthiophene) (P3HT) as a standard electron donor material, combined with phenyl-C<sub>61</sub>-butyric acid methyl ester (PC<sub>61</sub>BM) as the electron acceptor.<sup>2</sup> The synthetic availability of P3HT and its ability to form semicrystalline lamellar microstructures that favour charge transport are major advantages for this application.<sup>3</sup> However, its weak absorption in some parts of the visible region and in the near-infrared limits the PCE of P3HT-based devices to about 5%.<sup>4</sup> To overcome this challenge, electron donor materials absorbing significant portions of the solar spectrum, in particular at longer wavelengths, are required. An interesting solution consists of combining a dye (polymer/small molecule) with an absorption spectrum complementary to that of P3HT, either by using a ternary blend active layer (P3HT/dye/PCBM)<sup>5</sup> or by incorporating the dye directly into the polymer backbone.<sup>6,7</sup>

As chromophores, porphyrins are ubiquitous in solar energy conversion devices due to their significant optical absorption and photochemical stability, which can be tuned through judicious modifications of their molecular structure.<sup>8</sup> An increase in the photocurrent was found in BHJ solar cells using porphyrins directly blended with polythiophenes<sup>9</sup> or covalently incorporated in the polymer backbone.<sup>6</sup> However, the natural tendency of porphyrins to aggregate can modify the ordered morphology of P3HT, thus negatively impacting the transport of photogenerated charges and decreasing the final PCE.<sup>6a,9c</sup> To address this limitation, end-group modification of the P3HT chains has emerged as a promising strategy to simultaneously control the active-layer morphology and improve the performance of PSCs.<sup>10</sup> Using living chain-growth Kumada Catalyst Transfer Polymerization (KCTP), perfect control over the end-groups on the conjugated polymer can be achieved.<sup>11</sup>

Here, we report the end-functionalization of P3HT with a controllable number of  $\pi$ -extended porphyrin units using KCTP. Takashi *et al.* previously reported that aryl isocyanide bearing a porphyrin pendant group can be converted quantitatively into the corresponding poly(aryl isocyanide).<sup>12</sup> More recently, well-defined block copolymers containing P3HT and poly(isocyanide) blocks were synthesized in a one-pot procedure.<sup>13</sup> Although the two block polymerizations are mechanistically distinct, the successive polymerization mediated by a common catalyst, proceeded in a controlled manner and led to block copolymers with tuneable molecular weights and compositions.<sup>13</sup> Here, by combining these strategies, the modification of the P3HT end-groups by  $\pi$ -extended porphyrins is pursued. To ensure good solubility of the final material, the number of porphyrin units attached to the P3HT is limited to few units. The synthesized polymers are found to be soluble in many organic solvents, have significantly broader absorption spectra than pure P3HT and are able to self-assemble into organized microstructures in solution and the solid-state. The effect of the porphyrin:thiophene ratio on the optical, thermal and morphological properties of the polymer is also discussed.

The isocyanide-based porphyrin monomer **1** was synthesized in three steps from the enaminoporphyrin **NH-NiTPP**, which was previously reported by Callot, Ruppert *et al.* (Scheme 1).<sup>14</sup> Due to the

<sup>a</sup> Institut Charles Gerhardt, Laboratoire de Chimie Moléculaire et d'Organisation du Solide (CMOS), Université de Montpellier 2, Place Eugène Bataillon, 34095 Montpellier Cedex 05, France, E-mail: sebastien.clement02@univ-montp2.fr; Tel: +33 467143971

<sup>b</sup> Service des Matériaux Polymères et Composites (SMPC), Centre d'Innovation et de Recherche en Matériaux et Polymères (CIRMAP), Université de Mons, 20 Place du Parc, 7000 Mons, Belgium.

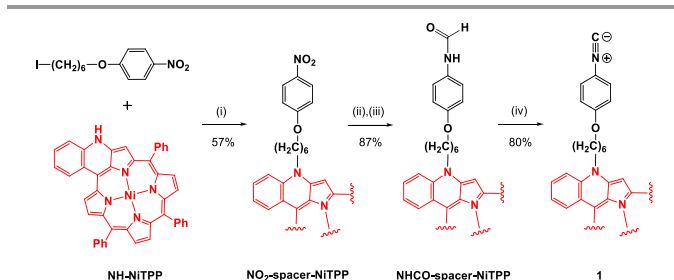
<sup>c</sup> Laboratory for Chemistry of Novel Materials, CIRMAP, University of Mons UMONS, Place du Parc 20, 7000 Mons, Belgium.

<sup>d</sup> School of Chemistry, Trinity College Dublin, the University of Dublin, Dublin 2, Ireland.

<sup>e</sup> Centre for Research on Adaptive Nanostructures and Nanodevices (CRANN), Trinity College Dublin, the University of Dublin, Dublin 2, Ireland.

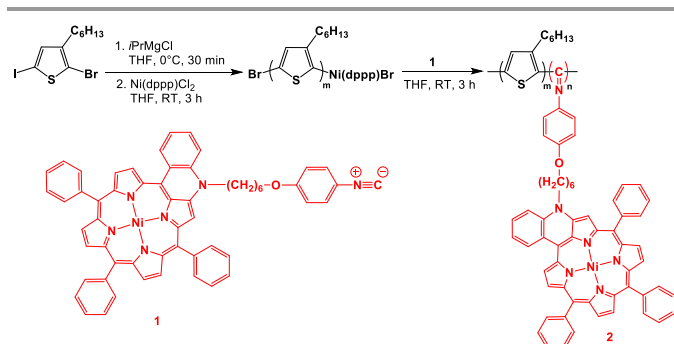
† Footnotes relating to the title and/or authors should appear here.  
Electronic Supplementary Information (ESI) available: materials and synthesis, NMR, GPC, IR, UV, TGA, DSC, XRD. See DOI: 10.1039/x0xx00000x

extension of the  $\pi$ -system of the porphyrin over the cyclized phenyl ring and the enamine, **NH-NITPP** exhibits a much broader absorption spectrum compared to other non-functionalized *meso*-tetraarylporphyrins (e.g. see Fig. S22, ESI<sup>†</sup>). *N*-alkylation of **NH-NITPP** with 1-(6-iodohexyloxy)-4-nitrobenzene afforded the corresponding **NO<sub>2</sub>-Spacer-NITPP** derivative. The reduction of the nitro group with sodium borohydride (NaBH<sub>4</sub>) and palladium on carbon (Pd/C 10 %), followed by formylation with formic acid, afforded **NHCO-spacer-NITPP** in 87 % yield. Subsequent dehydration with POCl<sub>3</sub>-NEt<sub>3</sub> afforded the desired isocyanide-based porphyrin monomer **1** in 80 % yield, which was fully characterized by mass spectrometry and NMR, IR and UV-Vis absorption spectroscopies (see ESI<sup>†</sup>).



**Scheme 1.** Synthesis of isocyanide-based porphyrin monomer **1**. Conditions: (i) NaH, THF, 25°C 2h, reflux 16h; (ii) NaBH<sub>4</sub>, Pd/C 10 %, CH<sub>2</sub>Cl<sub>2</sub>/CH<sub>3</sub>OH, 25°C 1h; (iii) formic acid, toluene, reflux 16h; (iv) POCl<sub>3</sub>, NEt<sub>3</sub>, THF, 0°C 3h.

With **1** in hand, its sequential copolymerization with 5-chloromagnesio-2-bromo-3-hexylthiophene was investigated (Scheme 2). Using standard KCTP methods, the P3HT macroinitiator with a living nickel end-group (Ni(dppp)Br) was synthesized. The polymerization was followed using Gel Permeation Chromatography (GPC) by removing aliquots from the polymerization mixture. When polymerization of the P3HT block was considered to be achieved, a solution of **1** (0.01 M) in THF was added to the reaction mixture. The orange P3HT solution immediately turned green and subsequently, turned to brown suggesting that copolymerization took place. After 3 hours, the solution was rapidly quenched with HCl (5 M) to prevent the interchain coupling reactions from occurring, and thus, to maintain a narrow dispersity.<sup>15</sup>



**Scheme 2.** Synthesis of P3HT end-functionalised with  $\pi$ -extended porphyrin in a one-pot procedure *via* sequential monomer addition.

GPC analysis of the isolated material revealed a higher number-averaged molecular weight ( $M_n$ ) for **2** compared to the P3HT macroinitiator (Fig. S20, ESI<sup>†</sup>), indicating successful chain growth polymerization. Both traces present monomodal, symmetric peaks, showing that no chain termination or chain transfer took place

during the polymerization. Completion of the polymerization was also inferred from IR spectroscopy, since the isocyanide band of the monomer **1** at  $\nu = 2118 \text{ cm}^{-1}$  disappeared in the IR spectrum of **2** (Fig. S21, ESI<sup>†</sup>).<sup>13,16</sup> As summarized in Table 1, three P3HTs end-functionalised with  $\pi$ -extended porphyrins with different  $M_n$  and compositions were synthesized by varying the initial ratio of the aforementioned monomers and catalyst. All synthesized polymers were isolated in good yields (>60 % over two steps) with narrow dispersity (<1.4). Their compositions were determined from the <sup>1</sup>H NMR spectra (Fig. S14, S16 and S18, ESI<sup>†</sup>) by integrating the signals observed at  $\delta = 0.90$  (terminal methyl group the hexyl side group of P3HT) and between  $\delta = 7.30$  and 9.00 ppm ( $\beta$ -pyrrolic and *meso* phenyl protons of the porphyrins.) As desired, the GPC data indicate that only a few porphyrin units (3-4) are incorporated as end-groups on the P3HT chains.

**Table 1.** Molecular weight and dispersity data for P3HT macroinitiators and the corresponding P3HT end-functionalised with  $\pi$ -extended porphyrin.

	P3HT		<b>2</b>		Yield (%)	Molar <b>3HT/1</b> ratio <sup>c</sup>
	$M_n$ (kDa) <sup>a,b</sup>	$M_w/M_n$ <sup>a,b</sup>	$M_n$ (kDa) <sup>b</sup>	$M_w/M_n$ <sup>b</sup>		
<b>2a</b>	8.0	1.28	12.2	1.39	70	90/10
<b>2b</b>	5.6	1.09	9.2	1.28	62	86/14
<b>2c</b>	1.7	1.24	5.0	1.18	60	68/32

<sup>a</sup>  $M_n$  and  $M_w/M_n$  of the P3HT moiety were determined by GPC analysis of aliquots removed from the reaction mixture before the addition of **1**. <sup>b</sup>  $M_n$  and  $M_w/M_n$  are reported as their polystyrene equivalents. <sup>c</sup> The molar ratio between 3-hexylthiophene (**3HT**) and **1** repeating units was determined by <sup>1</sup>H NMR spectroscopy in CDCl<sub>3</sub>.

The optical properties of **2** were subsequently investigated. In chloroform, the UV-Vis absorption spectra of polymers **2a-c** are very similar to that of the isocyanide-based porphyrin monomer **1** (Fig. S22, ESI<sup>†</sup>), with a strong absorption band between 420 and 450 nm and weaker absorption bands between 550 and 636 nm assigned to the Soret and Q bands of **1**, respectively. In addition, the absorption band appears broader in the 350-450 nm region due to the concomitant P3HT absorption. Usually, P3HT can be directed to self-assemble into crystalline nanowires by adding a nonsolvent to a polymer dissolved in a good solvent.<sup>17</sup> Thus, the optical properties of **2** were studied in chloroform/methanol mixtures at different ratios. Polymer **2a** was initially dissolved in chloroform, a good solvent for both P3HT and porphyrin moieties, and aggregation was subsequently induced by adding methanol (MeOH) in increasing ratios. Upon MeOH addition, the colour of the solution turned from green to brown, indicating self-assembly of the polymer chains (Fig. 1). Moreover, further increasing the MeOH content results in a gradual decrease in the absorbance at 426 and 447 nm and the growth of vibronic bands at 518, 556, 601 and 636 nm (Fig. 1). An isobestic point is observed at 480 nm, indicating that two distinct species, *i.e.* isolated polymer chains and aggregates, contribute to the absorption profile in mixtures from 10/0 to 3/7 (CHCl<sub>3</sub>/MeOH, v/v).<sup>17</sup> These results indicate interchain  $\pi$ - $\pi$  interactions associated with the formation of semicrystalline aggregates. Dynamic light scattering (DLS) measurements of polymer **2a** in CHCl<sub>3</sub>/MeOH (1:1) revealed that nanostructures with a monomodal size distribution (Figure S25, ESI<sup>†</sup>) were formed. The hydrodynamic diameter of the aggregates was found to be  $151 \pm 26 \text{ nm}$ .

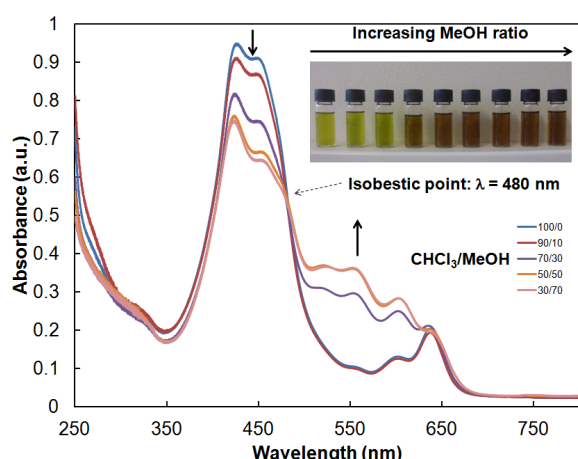


Fig. 1. Photographs and UV-Vis absorption spectra of **2a** in chloroform/methanol mixtures from 10/0 to 3/7 ( $\text{CHCl}_3/\text{MeOH} = v/v$ ,  $C = 0.06 \text{ mg mL}^{-1}$ ).

To investigate the self-assembly of the polymer chains in the solid state in more details, the UV-vis absorption of polymer thin films were recorded and compared to P3HT and porphyrin **1** thin films (Fig. S23, ESI<sup>†</sup>). As observed in  $\text{CHCl}_3/\text{MeOH}$  (1:1), polymer **2a** thin film exhibits vibronic structure with notably, shoulder peaks at approximately, 520, 550 and 600 nm. These peaks correspond fairly well with those observed in pristine P3HT thin films indicating that the bulky porphyrin end groups does not seem to disrupt the packing of the P3HT chains.<sup>10a</sup>

The influence of the P3HT:porphyrin molar ratio on the optical and self-assembly properties was then studied. The UV-Vis absorption spectra of **2a** and **2b** in the solid state exhibit the same profile but with a lower absorbance between 500 and 700 nm due to the higher porphyrin content (Fig. S24, ESI<sup>†</sup>). In contrast, the absorption profile of **2c** appears to be almost identical to that of the porphyrin monomer **1** and exhibits no vibronic band between 500 and 600 nm. This indicates that introducing an excessive number of porphyrin units prevents intermolecular interactions between polymer chains, leading to a reduction in overlap through  $\pi$ - $\pi$  stacking and disturbed arrangement in the solid films.<sup>19</sup> Thus, while the incorporation of  $\pi$ -extended porphyrin units into the P3HT chain-ends enables the absorption profile of the polymer material to be significantly extended, the porphyrin:P3HT ratio must be kept low enough to avoid the loss of the supramolecular organisation of the P3HT segments in the solid state.

To investigate the effect of the porphyrin molar ratio on the thermal properties, thermogravimetric analysis (TGA) and differential scanning calorimetry (DSC) measurements were performed under an inert atmosphere at a heating rate of  $10^\circ \text{C min}^{-1}$ . Polymers **2a-c** display excellent thermal stability, with the first weight losses upon heating occurring only at temperatures exceeding  $330^\circ \text{C}$  (Fig. S26, ESI<sup>†</sup>). The DSC measurements show different thermal transitions, depending on the porphyrin:P3HT ratio (Fig. S27, ESI<sup>†</sup>): introduction of the porphyrin leads to a decrease in the melting and, to a lesser extent, crystallization temperatures in comparison with the neat P3HT.<sup>20</sup> Upon cooling, a crystallization temperature of  $115^\circ \text{C}$  (compared to  $200^\circ \text{C}$  for P3HT) and, upon heating, a melting temperature of  $206^\circ \text{C}$  (compared to  $210^\circ \text{C}$  for P3HT) are found for **2a**. The melting and crystallization temperatures of polymer **2b** are

lower than for **2a**, whereas polymer **2c** appears to be fully amorphous. The evolution is a consequence of the increasing porphyrin molar ratio when going from **2a** to **2c**. These results are consistent with the observed changes in UV-Vis absorption spectra and confirm that the porphyrin:P3HT ratio needs to be carefully controlled to retain the semicrystalline nature of P3HT.

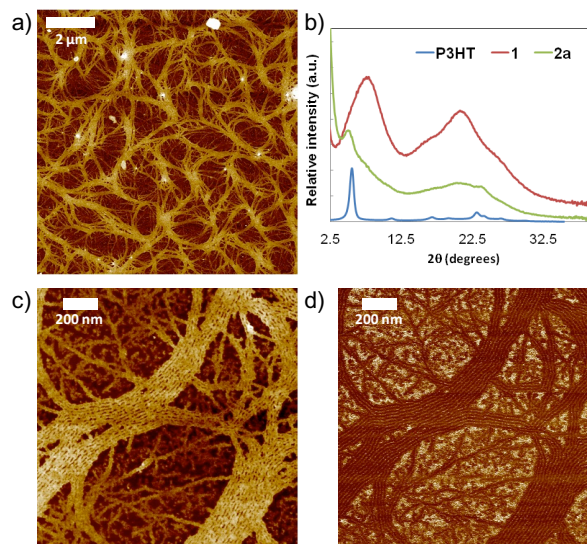


Fig. 2. (a)  $10 \times 10 \mu\text{m}^2$  Peak Force AFM height image of **2a** drop-cast from xylene onto a mica substrate; (b) X-ray diffraction pattern of isocyanide porphyrin monomer **1**, P3HT and **2a**; (c,d)  $1.5 \times 1.5 \mu\text{m}^2$  Peak Force AFM height (c) and DMT modulus (d) images of **2a** showing the fibrillar morphology.

To analyze the microscopic morphology of the polymers in the solid state, Atomic Force Microscopy (AFM) in the Peak Force Tapping mode was performed. Polymer **2a** is the only sample with a well-defined nanostructured morphology. At a scale of  $10 \mu\text{m}$  (Fig. 2a), we observe a web of few hundred nm-wide tapes. These tapes are composed of aligned fibrils, which can extend over a few micrometers in length (Fig. 2c and 2d). This fibrillar nanoscale morphology is characteristic of highly regioregular P3HT.<sup>21</sup> Powder X-ray diffraction (XRD) measurements were also performed on polymer **2a** and confirm the microstructure (Fig. 2b). The diffraction pattern exhibits reflections assigned to pristine P3HT and isocyanide porphyrin monomer **1**, indicating the retention of the crystalline structures inherent to both components. The peak at  $2\theta \sim 5.0^\circ$  is typical of a lamellar structure is observed in the P3HT diffraction pattern ( $2\theta \sim 5.5^\circ$ ).<sup>22</sup> In addition, the broad reflection centered at  $2\theta \sim 20.3^\circ$  can be related to diffraction from the isocyanide porphyrin monomer **1** ( $2\theta \sim 20.8^\circ$ ), which corresponds to the  $\pi$ - $\pi$  stacking distance ( $2.8 \text{ \AA}$ ) between two porphyrin units. These similarities, in particular the position of the (100) lattice peak, indicate that the porphyrin moiety, if maintained in relatively low quantity, does not affect the P3HT crystallite structure.

In summary, P3HTs end-functionalized with  $\pi$ -extended porphyrin have been synthesized using a one-pot procedure based on the distinct polymerization of thiophene and  $\pi$ -extended porphyrin monomers functionalized with a pendant arylisocyanide group. By judiciously adjusting the P3HT:porphyrin molar ratio, self-assembly of the end-functionalized P3HT chains can be achieved, leading to broader absorption profile while maintaining fibrillar nanoscale

morphology. The extended visible absorption window, combined with the tunable thin film morphology suggest that these polymers may demonstrate considerable potential as electron donor materials in BHJ polymer solar cells. Further outcoming studies will investigate in more details the aggregation and the self-assembling properties of these polymers and their influence on the photovoltaic performance.

The authors thank the CNRS and the Université de Montpellier for financial support. Research in Mons is supported by the Science Policy Office of the Belgian Federal Government (BELSPO; PAI 7/05), FNRS-FRFC and Région Wallonne (OPTI2MAT excellence programme). The authors are also grateful to National Fund for Scientific Research (F.R.S.-FNRS) in the frame of the FRFC research program (convention no. 2.4508.12).

## Notes and references

- (a) L. Yang, H. Zhou, A. C. Stuart and W. You in *Organic Photovoltaics* (2<sup>nd</sup> edition), ed. C. J. Brabec, U. Scherff and V. Dyakonov, Wiley-VCH, Weinheim, 2014, 61; (b) J. Youa, L. Doua, Z. Hong, G. Lia, Y. Yang, *Prog. Polym. Sci.*, 2013, **38**, 1909; (c) G. Li, R. Zhu, Y. Yang, *Nature Photonics*, 2012, **6**, 153.
- M. T. Dang, L. Hirsch, and G. Wantz, *Adv. Mater.*, 2011, **23**, 3597.
- (a) I. Osaka and R. D. McCullough, *Acc. Chem. Res.*, 2008, **41**, 1202; (b) *Handbook of Oligo- and Polythiophenes*; ed. D. Fichou, Wiley VCH: Weinheim, 2007.
- (a) C. J. Brabec, S. Gowrisanker, J. J. M. Halls, D. Laird, S. Jia and S. P. Williams, *Adv. Mater.*, 2010, **22**, 3839; (b) G. Dennler, M. C. Scharber and C. J. Brabec, *Adv. Mater.*, 2009, **21**, 1323.
- (a) F. Goubard and G. Wantz, *Polym. Int.* 2014, **63**, 1362; (b) Y.-C. Chen, C.-Y. Hsu, R. Y.-Y. Lin, K.-C. Ho and J. T. Lin, *ChemSusChem*, 2013, **6**, 20.
- (a) L. Angiolini, V. Cocchi, M. Lanzi, E. Salatelli, D. Tonelli, Y. Vlamidis, *Mater. Chem. Phys.*, 2014, **146**, 464; (b) L. Angiolini, T. Benelli, V. Cocchi, M. Lanzi and E. Salatelli, *React. Funct. Polym.*, 2013, **73**, 1198.
- (a) J. U. Lee, Y. D. Kim, J. W. Jo, J. P. Kim and W. H. Jo, *J. Mater. Chem.*, 2011, **21**, 17209; (b) B. J. Campo, J. Duchateau, C. R. Ganivet, B. Ballesteros, J. Gilot, M. M. Wienk, W. D. Oosterbaan, L. Lutsen, T. J. Cleij, G. de la Torre, R. A. J. Janssen, D. Vanderzande and T. Torres, *Dalton Trans.*, 2011, **40**, 3979.
- (a) J. Kesters, P. Verstappen, M. Kelchtermans, L. Lutsen, D. Vanderzande and W. Maes, *Adv. Energy Mater.* 2015, DOI: 10.1002/aenm.201500218; (b) K. M. Kadish, K. M. Smith, R. Guilard, *The Porphyrin Handbook Vol. 6*, Academic Press: New York, 2000.
- (a) H. Xu, H. Ohkita, T. Hirata, H. Benten and S. Ito, *Polymer*, 2014, **55**, 2856; (b) D. M. Lyons, J. Kesters, W. Maes, C. W. Bielawski and J. L. Sessler, *Synth. Met.*, 2013, **178**, 56; (c) D. M. Lyons, R. J. Ono, C. W. Bielawski and J. L. Sessler, *J. Mater. Chem.*, 2012, **22**, 18956.
- (a) S. L. Fronk, C.-K. Mai, M. Ford, R. P. Noland and G. C. Bazan, *Macromolecules*, 2015, DOI: 10.1021/acs.macromol.5b00986; (b) Z. Mao, K. Vakhshouri, J. Chernov, D. A. Fischer, R. Fernando, D. M. DeLongchamp, E. D. Gomez and G. Sauve, *Macromolecules*, 2013, **46**, 103; (c) J. S. Kim, Y. Lee, J. H. Lee, J. H. Park, J. K. Kim and K. Cho, *Adv. Mater.*, 2010, **22**, 1355.
- (a) N. V. Handa, A. V. Serrano, M. J. Robb and C. J. Hawker, *J. Polym. Sci A Polym. Chem.*, 2015, **53**, 831; (b) R. H. Lohwasser and M. Thelakktat, *Macromolecules*, 2011, **44**, 3388; (c) A. Smeets, K. Van den Bergh, J. De Winter, P. Gerbaux, T. Verbiest and G. Koeckelberghs, *Macromolecules*, 2009, **42**, 7638.
- F. Takei, K. Onitsuka, N. Kobayashi and S. Takahashi, *Chem. Lett.*, 2000, 914.
- (a) M. Su, S.-Y. Shi, Q. Wang, N. Liu, J. Yin, C. Liu, Y. Ding and Z.-Q. Wu, *Polym. Chem.*, 2015, **6**, 6519; (b) R. J. Ono, A. D. Tood, Z. Hu, D. A. Vanden Bout and C. W. Bielawski, *Macromol. Rapid. Commun.*, 2013, **35**, 204; (c) Z.-Q. Wu, J. D. Radcliffe, R. J. Ono, Z. Chen, Z. Li and C. W. Bielawski, *Polym. Chem.*, 2012, **3**, 874; (d) N. Liu, C.-G. Qi, Y. Wang, D.-F. Liu, J. Yin, Y.-Y. Zhu and Z.-Q. Wu, *Macromolecules*, 2013, **46**, 7753. (e) Z.-Q. Wu, R. J. Ono, Z. Chen and C. W. Bielawski, *J. Am. Chem. Soc.*, 2010, **132**, 14000.
- S. Richeter, C. Jeandon, J.-P. Gisselbrecht, R. Graff, R. Ruppert and H. J. Callot, *Inorg. Chem.*, 2004, **43**, 251.
- R. Miyakoshi, A. Yokoyama, T. Yokozawa, *Macromol. Rapid. Commun.*, 2004, **25**, 1663.
- A. Thomas, J. E. Houston, N. Vand Den Brande, J. De Winter, M. Chevrier, R. K. Heenan, A. E. Terry, S. Richeter, A. Mehdi, B. Van Mele, P. Dubois, R. Lazzaroni, P. Gerbaux, R. C. Evans and S. Clément, *Polym. Chem.*, 2014, **5**, 3352.
- (a) E. Lee, B. Hammer, J.-K. Kim, Z. Page, T. Emrick, and R. C. Hayward, *J. Am. Chem. Soc.*, 2011, **133**, 10390; (b) L. G. Liu, G. H. Lu, X. N. Yang, *J. Mater. Chem.*, 2008, **18**, 1984.
- C. Scharsich, R. H. Lohwasser, M. Sommer, U. Asawapirom, U. Scherf, M. Thelakktat, D. Neher and A. Köhler, *J. Polym. Sci., Polym. Phys.*, 2012, **50**, 442.
- L. Wang, S. Shi, D. Ma, S. Chen, C. Gao, M. Wang, K. Shi, Y. Li, X. Li, H. Wang, *Macromolecules*, 2015, **48**, 287.
- (a) P. Koh, S. Huettner, H. Komber, V. Senkovskyy, R. Tkachov, A. Kiriy, R. H. Friend, U. Steiner, W. T. S. Huck, J.-U. Sommer and M. Sommer, *J. Am. Chem. Soc.*, 2012, **134**, 4790; (b) D. E. Motaung, G. F. Malgas, C. J. Arendse, S. E. Mavundla, C. J. Oliphant, D. Knoesen, *Sol. Energ. Mat. Sol. Cells*, 2009, **93**, 1674.
- (a) H. Yang, T. J. Shin, L. Yang, K. Cho, C. Y. Ryu and Z. Bao, *Adv. Funct. Mater.* 2005, **15**, 671; (b) M. Surin, S. Cho, J. D. Yuen, G. Wang, K. Lee, P. Leclère, R. Lazzaroni, D. Moses, A. J. Heeger, *J. Appl. Phys.*, 2006, **100**, 33712 ; (c) S. Berson, R. De Bettignies, S. Bailly, S. Guillerez, *Adv. Funct. Mater.*, 2007, **17**, 1377.
- (a) T. J. Prosa, M. J. Winokur, J. Moulton, P. Smith, A. J. Heeger, *Macromolecules*, 1992, **25**, 4364; (b) K. Tashiro, K. Ono, Y. Minagawa, M. Kobayashi, T. Kawai, K. Yoshino, *J. Polym. Sci., Part B: Polym. Phys.* 1991, **29**, 1223.